

# Joint learning of images and videos with a single Vision Transformer

Shuki Shimizu  
Nagoya Institute of Technology  
Nagoya, Japan  
s.shimizu.562@nitech.jp

Toru Tamaki  
Nagoya Institute of Technology  
Nagoya, Japan  
tamaki.toru@nitech.ac.jp

## Abstract

In this study, we propose a method for jointly learning of images and videos using a single model. In general, images and videos are often trained by separate models. We propose in this paper a method that takes a batch of images as input to Vision Transformer (IV-ViT), and also a set of video frames with temporal aggregation by late fusion. Experimental results on two image datasets and two action recognition datasets are presented.

## 1 Introduction

Image and action recognition are long-standing tasks and have been studied extensively. Many deep learning models for image recognition have been proposed [4, 7, 18, 38, 41], and many datasets for image recognition have been made publicly available [6, 25]. Action recognition also has a long history [15, 21, 48], with large datasets [24, 26, 39] and various models [2, 5, 11, 12, 16, 37, 42, 47] proposed.

With the rapid growth of Vision Transformer (ViT) [7] in recent years, research on learning a multi-modal model for images and videos has emerged [10, 13, 14, 27]. Although many CNN-based image and action recognition models have been proposed, most of them were developed separately because of the modality difference between images and videos in terms of temporal modeling. As ViT became popular, action recognition models based on ViT were proposed [35]. ViT divides an image into patches and applies Transformer [44] by considering the patches as tokens, while ViT-based action recognition models divide a video into patches. This structure allows models to simplify the model design by providing both images and videos in a similar way [14, 27].

However, prior works have not fully exploited the relation of image and video modalities; an image is considered a video with one frame, while a video is a series of frames. In this paper, we propose *IV-ViT*, a model for joint learning of images and videos with a single ViT model with a maximal parameter sharing. The proposed method shown in Fig. 1 applies a ViT to each frame, which is a frame-wise ViT often used as a

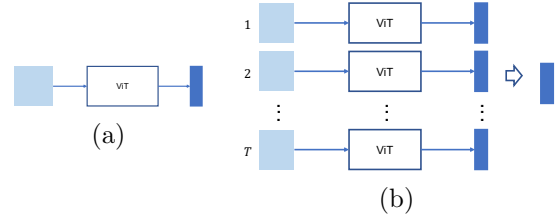


Figure 1: The proposed IV-ViT for cases (a) when input is an image, and (b) when input is a video clip of  $T$  frames.

baseline of action recognition [17, 47]. When recognizing a batch of images, ViT is simply applied, and when recognizing a video, the output of ViT for each frame of the video is aggregated by late fusion [19]. This structure enables joint learning of images and videos using a single ViT model. To enable the frame-wise model to handle the temporal information, we utilize the temporal feature shift [17, 28, 47] by interacting features between neighbor frames.

## 2 Related work

### 2.1 Image and action recognition

Since ImageNet [6], many CNN models [18, 23, 38, 41] and recently ViT models [7, 29] have been proposed for image recognition. There has also been a lot of research on action recognition based on 3D CNN [5, 11, 12, 16, 42] and ViT [2, 32, 36, 47].

For efficient modeling of temporal information with 3D CNN, some works used spatio-temporal separable convolutions instead of fully 3D convolutions [34, 43, 46], and others introduced temporal feature shift in frame-wise (or 2D CNN-based) models [9, 28, 40]. ViT-based video models have the self-attention mechanism to model the temporal information, such as using transformer for late-fusion [32, 36], separate spatial and temporal attentions [2], or restricted spatio-temporal attention [3, 4], and feature shift [17, 47].

### 2.2 Joint learning of images and videos

Several attempts have been made to recognize both images and videos with a single model even using CNN.

UniDual [45] and Omnisorce [8] used 3D CNN models [12, 43] for both videos and images by first replicating a still image  $T$  times and then converting them to a 3D volume of  $T$  frames, which is inefficient for learning images.

Unlike CNN, ViT uses patch embeddings, which makes it easier to handle different modalities in a unified manner. PolyViT [27] and Omnivore [14] simultaneously learn multi-modal data including images, videos, and audio [27] or RGB+Depth [14].

Omnivore [14] uses the same embedding layer for both images and videos, however, by zero-padding to a still image  $T$  times and then converting them to a 3D volume of  $T$  frames, which is as inefficient as [8, 45]. PolyViT [27] uses different embedding layers for different modalities, even for images and videos, although both are the same visual modality.

In contrast, our method, IV-ViT, shares the same embedding layer for images and videos like as Omnivore [14], but without converting images into 3D volumes by replication or zero-padding. Instead, we train a single model for a batch of images and a batch of video frames in the same manner, as explained below.

### 3 ViT model

In this section, we give a brief introduction to ViT for images [7] and a frame-wise ViT for videos [47].

#### 3.1 Image

Let  $x \in \mathbb{R}^{3 \times H \times W}$  be an input image, where  $H$  and  $W$  are the height and width of the image. The input image is first divided into  $P \times P$  pixel patches and transformed into a tensor  $\hat{x} = [x_0^1, \dots, x_0^N] \in \mathbb{R}^{N \times d}$ , where  $x_0^i \in \mathbb{R}^d$  is the  $i$ -th patch,  $N = \frac{HW}{P^2}$  is the number of patches, and  $d = 3P^2$  is the patch dimension. The input patch  $x_0^i$  is transformed by a linear transformation using the  $D$ -dimensional embedding matrix  $E$  and the addition of the positional embedding  $E_{\text{pos}}$  as follows;

$$z_0 = [c_0, x_0^1 E, x_0^2 E, \dots, x_0^N E] + E_{\text{pos}}, \quad (1)$$

where  $c_0 \in \mathbb{R}^D$  is a class token. This patch embedding  $z_0 \in \mathbb{R}^{(N+1) \times D}$  is input to the first encoder block  $M^\ell$  of the transformer, in which the self-attention mechanism is applied to patches. Let  $z_\ell$  be the input to the  $\ell$ -th block  $M^\ell$  and  $z_\ell$  be the output;

$z_\ell = M^\ell(z_{\ell-1})$ . Then, the output  $z_L$  of ViT consisting of  $L$  blocks is

$$z_L = (M^L \circ \dots \circ M^1 \circ M^0)(x) \in \mathbb{R}^{(N+1) \times D}. \quad (2)$$

Note that  $\circ$  is the composition and  $M^0$  is the embedding layer. The final head  $M^h(z_L)$

often uses the part of  $z_L$  corresponding to the class token only;

$\tilde{z}_{L,d} = z_{L,0,d}$ , where  $(n,d)$  elements of  $z_\ell$  is denoted by  $z_{\ell,n,d}$ . Then the class prediction is

$$\hat{y} = M^h(\tilde{z}_L) \in [0, 1]^C, \quad (3)$$

where  $C$  is the number of categories.

#### 3.2 Video

Let  $x \in \mathbb{R}^{T \times 3 \times H \times W}$  be an input video clip where  $T$  is the number of frames in the video clip. Each frame is transformed separately into patches like images.

The differences are the dimension of the class token  $c_0 \in \mathbb{R}^{T \times D}$  and patch embeddings  $z_0 \in \mathbb{R}^{T \times (N+1) \times D}$ . The output  $z_L$  of the same ViT with  $L$  blocks  $M^\ell$  ( $\ell = 0, \dots, L$ ) is as follows.

$$z_L = (M^L \dots M^1 \circ M^0)(x) \in \mathbb{R}^{T \times (N+1) \times D}. \quad (4)$$

We use a simple average pooling [17, 47] for temporal aggregation to summarize outputs from each frame of the video. Let  $(t,n,d)$  elements of  $z_\ell$  be denoted by  $z_{\ell,t,n,d}$  and  $\tilde{z}_\ell \in \mathbb{R}^{T \times D}$  corresponding to the class token be denoted by  $\tilde{z}_{\ell,t,d}$ . The class token  $\tilde{z}_{L,t,d} = z_{L,t,0,d}$  is aggregated by

$$\bar{z}_{L,d} = \frac{1}{T} \sum_t \tilde{z}_{L,t,d}, \quad (5)$$

and the head  $M^h$  predicts the category by

$$\hat{y} = M^h(\bar{z}_L) \in [0, 1]^C. \quad (6)$$

## 4 Proposed IV-ViT Model

#### 4.1 Model input

The above ViT for images and videos can be handled in a consistent manner. In general when training with images, a batch of images  $x \in \mathbb{R}^{B \times 3 \times H \times W}$  of size  $B$  is used as input, and the output  $\hat{y} \in [0, 1]^{B \times C}$  is for the batch. In other words, the shape of input/output of ViT blocks  $M_\ell$  is the same for images and videos, and the ViT blocks do not need to distinguish whether the input is video frames or a batch of images. That is, the output of the  $\ell$ -th block is  $z_\ell \in \mathbb{R}^{B \times (N+1) \times D}$  for a batch of images, and  $z_\ell \in \mathbb{R}^{BT \times (N+1) \times D}$  for a batch of video frames. Therefore, the same ViT architecture can be used for images and videos, including the embedding layer.

**Images:** Take a batch of images  $x \in \mathbb{R}^{B \times 3 \times H \times W}$  as input. The output of the  $L$ -th block is  $z_L \in \mathbb{R}^{B \times (N+1) \times D}$ , and the class token  $\tilde{z}_L \in \mathbb{R}^{B \times D}$  is used to predict  $\hat{y} \in [0, 1]^{B \times C}$  by the head. This is a common case when training a ViT for images.

**Videos:** Take a batch of video clips  $x \in \mathbb{R}^{B \times T \times 3 \times H \times W}$  as input. To input this 5D tensor to ViT, the time dimension is expanded to the

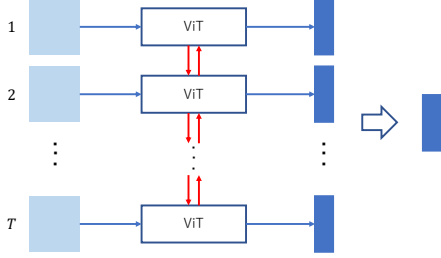


Figure 2: Concept of feature shift between ViT modules in successive frames.

batch dimension and transformed into a 4D tensor  $x' \in \mathbb{R}^{BT \times 3 \times H \times W}$ . The output of the  $L$ -th block  $z_L \in \mathbb{R}^{BT \times (N+1) \times D}$  is first transformed into  $z'_L \in \mathbb{R}^{B \times T \times (N+1) \times D}$ . Then, the class token part  $\tilde{z}'_L \in \mathbb{R}^{B \times T \times D}$  is extracted and average pooling over the time dimension is applied to obtain  $\bar{z}'_L \in \mathbb{R}^{B \times D}$ . The output by the head is  $\hat{y} \in [0, 1]^{B \times C}$ .

## 4.2 Modeling of temporal information

The proposed IV-ViT model uses a frame-wise ViT for videos, which is not sufficient to model the temporal information of the video. Therefore, we introduce the feature shift [4, 17, 47] that can handle temporal information while maintaining the structure, as shown in Fig. 2.

For the frame dimension  $t$  of features  $z_{t,n,d}^\ell$  in the  $\ell$ -th block  $M^\ell$ , we shift elements between successive frames  $t+1$  and  $t-1$  by a certain amount  $D_b$  and  $D_f$  as follows.

$$z_{\text{out},t,0,d}^\ell = \begin{cases} z_{\text{in},t-1,0,d}^\ell, & 1 < t \leq T, 1 \leq d < D_b \\ z_{\text{in},t+1,0,d}^\ell, & 1 \leq t < T, D_b \leq d < D_b + D_f \\ z_{\text{in},t,0,d}^\ell, & \forall t, D_b + D_f \leq d \leq D \end{cases} \quad (7)$$

$$z_{\text{out},t,n,d}^\ell = z_{\text{in},t,n,d}^\ell, \quad \forall t, 1 \leq n < N, \forall d, \quad (8)$$

where  $z_{\text{in},t,n,d}^\ell$  and  $z_{\text{out},t,n,d}^\ell$  are features  $z_{t,n,d}^\ell$  before and after the shift operation, which is the same as TokenShift [47].

In this way, one block shifts the information in the time direction for one time period. Therefore, it is possible to interact the temporal information of the whole clip by using the number of ViT blocks  $L$  larger than the clip length  $T$  [17].

## 5 Experimental results

### 5.1 Datasets

In our experiments, we used the following two image and two video datasets, in total four datasets.

- Tiny-ImageNet [1]: A subset of ImageNet [6] consisting of 100,000 training images and 10,000 validation images. Each training image is  $64 \times 64$  selected from 200 ImageNet classes (500 images per class).
- CIFAR-100 [22]: An image dataset consisting of 50,000 training images and 10,000 validation images. The number of categories is 100 and the size is  $32 \times 32$ .
- Mini-Kinetics (aka Kinetics200) [46]: A subset of Kinetics400 [20], an action recognition dataset, consisting of 78246 training videos and 5000 validation videos. Each video is selected from 200 classes of Kinetics400 (about 400 videos for each class).
- UCF101 [39]: A 101-class action recognition dataset consisting of 9537 training videos and 3783 validation videos.

### 5.2 Model

In experiments, we used ViT [7] pretrained on Kinetics400 [20] as a frame-wise ViT given by [47]. We followed TokenShift [47] for temporal feature shift. Hence the IV-ViT model has four heads for each dataset, while the same embedding layer is used for all datasets.

### 5.3 Training samples

For images, a crop was made with a random area in the range  $[0.08, 1.0]$  with respect to the area of the original image, and a random aspect ratio in the range  $[\frac{3}{4}, \frac{4}{3}]$ , and resize it to  $224 \times 224$  pixels. Then the crop was flipped horizontally with a probability of  $1/2$ .

For videos, a clip was created by extracting consecutive frames corresponding to a specified duration (2.67 seconds in experiments) from a video, and sampling  $T = 16$  frames uniformly from the extracted frames. The shorter edge of the extracted frame was randomly resized in the range of  $[224, 320]$  pixels while maintaining the aspect ratio. Then  $224 \times 224$  pixels at random locations were cropped and flipped horizontally with a probability of  $1/2$ .

Mini-batches were sampled from each dataset sequentially in a fixed order (Tiny-ImageNet, CIFAR100, UCF101, and mini-Kinetics), with the batch size of 6 for both image and video datasets. This means that a mini-batch of videos consists of 96 frames, since each of 6 video clips consists of 16 frames. When a mini-batch was sampled from each dataset, the gradient were computed and the parameters were updated. The number of iterations was set to 20k, each iteration includes updates by four datasets (so in total 80k iterations), and epochs for each dataset do not align as in [33]. The optimizer was AdamW [31] with the learning rate of  $1e-5$  and weight decay of  $5e-5$  for all datasets, although each dataset might have different optimal settings [27].

Table 1: Performance comparison for four image and video datasets. Note that averages for “IV-ViT (images/videos)” are for each domain.

|                   | pretrain  | Tiny-ImageNet |       | CIFAR100 |       | UCF101 |       | mini-Kinetics |       | average |       |
|-------------------|-----------|---------------|-------|----------|-------|--------|-------|---------------|-------|---------|-------|
|                   |           | top-1         | top-5 | top-1    | top-5 | top-1  | top-5 | top-1         | top-5 | top-1   | top-5 |
| IV-ViT            | K400      | 83.22         | 94.97 | 88.69    | 98.61 | 90.08  | 98.81 | 62.83         | 85.55 | 81.21   | 94.49 |
| IV-ViT (separate) | K400      | 83.10         | 95.18 | 88.89    | 98.71 | 89.34  | 98.89 | 62.71         | 85.03 | 81.01   | 94.45 |
| IV-ViT (images)   | K400      | 83.95         | 95.44 | 87.74    | 98.49 | –      | –     | –             | –     | 85.84   | 96.96 |
| IV-ViT (videos)   | K400      | –             | –     | –        | –     | 93.10  | 99.39 | 68.75         | 88.42 | 80.92   | 93.90 |
| PolyViT           | K400      | 80.82         | 94.18 | 86.33    | 98.20 | 92.23  | 99.02 | 71.49         | 89.98 | 82.72   | 95.34 |
| PolyViT           | K400+I21K | 80.29         | 93.84 | 86.36    | 97.88 | 91.88  | 98.84 | 71.68         | 89.74 | 82.55   | 95.07 |
| IV-ViT            | scratch   | 23.65         | 48.57 | 35.23    | 66.54 | 41.06  | 73.10 | 13.27         | 34.31 | 28.30   | 55.63 |
| PolyViT           | scratch   | 14.88         | 35.60 | 24.30    | 53.57 | 32.09  | 59.64 | 10.54         | 27.55 | 20.45   | 44.09 |

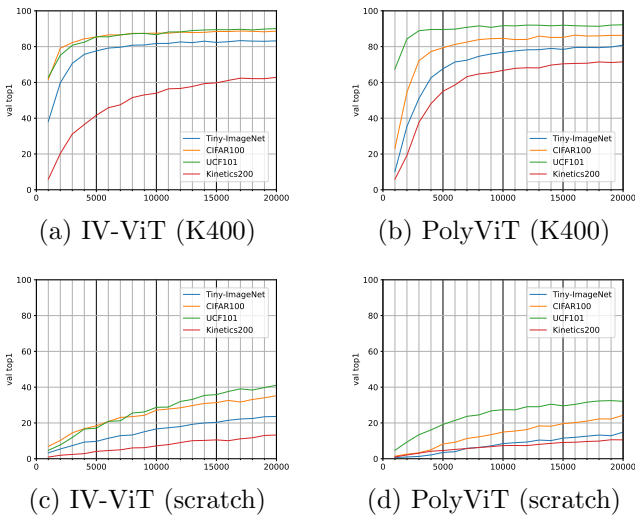


Figure 3: Training progress of our model and PolyViT with and without pretraining.

## 5.4 Results and comparison

Table 1 shows the performance comparison. The avg column shows the average of top-1/5 accuracy of four datasets. We compared the proposed IV-ViT to PolyViT [27] with our implementation. For PolyViT, we used the same Kinetics400-pretrained weights with IV-ViT for the image embedding layer and the transformer blocks, while we used Kinetics400-pretrained ViViT [2] for the video embedding layer. As an alternative, we added a version using ImageNet21k-pretrained weights for the image embedding layer, while others maintained. The training procedure was the same with IV-ViT, except the number of frames in a clip was 32 and the batch size was set to 3.

The proposed IV-ViT performs better than PolyViT for images, even when PolyViT uses ImageNet21k-pretrained weights for the image embedding layer. Our model, however, works worse for videos, in particular mini-Kinetics. This may be due to the use of the same embedding layer for images and videos in our

model, while PolyViT uses different embedding layers. However, as shown in the row “IV-ViT (separate)” of Tab. 1, our model still shows a similar performance even when separate (hence different) embedding layers for images and videos were used. Results of our model with either image datasets only or video datasets only are also shown in Tab. 1 in rows “IV-ViT (images)” and “IV-ViT (videos)”. The performance of IV-ViT for videos becomes better when training with videos only, while the performance for images doesn’t change when training with images only. This suggests the need for more investigation on training videos when jointly trained with images.

Another comparison with PolyViT shown in Table 1 is the training from scratch. For the fixed number of iterations, our IV-ViT is faster and easier to train. As seen in Fig. 3(d), the performance of PolyViT for UCF101 looks saturated indicating overfitting. In contrast, Fig. 3(c) shows that the performance increases steadily for all datasets, which demonstrates the effectiveness of the architecture of IV-ViT.

## 6 Conclusion

In this paper, we propose IV-ViT, a model that can handle images and videos in the same model, by adopting a frame-wise ViT with temporal feature shift. Our IV-ViT is limited to image and video modalities, however, allowing extensions in several ways. Future work includes the use of other temporal modeling such as TimeSformer [3] or VideoSwin [30] instead of feature shift, more sophisticated temporal fusion [32, 36] instead of average pooling, and tuning training procedures and hyperparameters for each dataset.

## Acknowledgement

This work was supported in part by JSPS KAKENHI Grant Number JP22K12090.

## References

- [1] Tiny imagenet. <https://www.kaggle.com/c/tiny-imagenet>, 2018. **3**
- [2] Anurag Arnab, Mostafa Dehghani, Georg Heigold, Chen Sun, Mario Lučić, and Cordelia Schmid. Vivit: A video vision transformer. In *Proceedings of the IEEE/CVF International Conference on Computer Vision (ICCV)*, pages 6836–6846, October 2021. **1, 4**
- [3] Gedas Bertasius, Heng Wang, and Lorenzo Torresani. Is space-time attention all you need for video understanding? In Marina Meila and Tong Zhang, editors, *Proceedings of the 38th International Conference on Machine Learning*, volume 139 of *Proceedings of Machine Learning Research*, pages 813–824. PMLR, 18–24 Jul 2021. **1, 4**
- [4] Adrian Bulat, Juan Manuel Perez Rua, Swathikiran Sudhakaran, Brais Martinez, and Georgios Tzimiropoulos. Space-time mixing attention for video transformer. In M. Ranzato, A. Beygelzimer, Y. Dauphin, P.S. Liang, and J. Wortman Vaughan, editors, *Advances in Neural Information Processing Systems*, volume 34, pages 19594–19607. Curran Associates, Inc., 2021. **1, 3**
- [5] Joao Carreira and Andrew Zisserman. Quo vadis, action recognition? a new model and the kinetics dataset. In *Proceedings of the IEEE Conference on Computer Vision and Pattern Recognition (CVPR)*, July 2017. **1**
- [6] Jia Deng, Wei Dong, Richard Socher, Li-Jia Li, Kai Li, and Li Fei-Fei. Imagenet: A large-scale hierarchical image database. In *2009 IEEE Conference on Computer Vision and Pattern Recognition*, pages 248–255, 2009. **1, 3**
- [7] Alexey Dosovitskiy, Lucas Beyer, Alexander Kolesnikov, Dirk Weissenborn, Xiaohua Zhai, Thomas Unterthiner, Mostafa Dehghani, Matthias Minderer, Georg Heigold, Sylvain Gelly, Jakob Uszkoreit, and Neil Houlsby. An image is worth 16x16 words: Transformers for image recognition at scale. In *International Conference on Learning Representations*, 2021. **1, 2, 3**
- [8] Haodong Duan, Yue Zhao, Yuanjun Xiong, Wentao Liu, and Dahua Lin. Omni-sourced webly-supervised learning for video recognition. *CoRR*, abs/2003.13042, 2020. **2**
- [9] Linxi Fan, Shyamal Buch, Guanzhi Wang, Ryan Cao, Yuke Zhu, Juan Carlos Niebles, and Li Fei-Fei. Rubiksnet: Learnable 3d-shift for efficient video action recognition. In Andrea Vedaldi, Horst Bischof, Thomas Brox, and Jan-Michael Frahm, editors, *Computer Vision – ECCV 2020*, Cham, 2020. Springer International Publishing. **1**
- [10] Quanfu Fan, Chun-Fu Chen, and Rameswar Panda. Can an image classifier suffice for action recognition? In *The Tenth International Conference on Learning Representations, ICLR 2022, Virtual Event, April 25–29, 2022*. OpenReview.net, 2022. **1**
- [11] Christoph Feichtenhofer. X3d: Expanding architectures for efficient video recognition. In *Proceedings of the IEEE/CVF Conference on Computer Vision and Pattern Recognition (CVPR)*, June 2020. **1**
- [12] Christoph Feichtenhofer, Haoqi Fan, Jitendra Malik, and Kaiming He. Slowfast networks for video recognition. In *Proceedings of the IEEE/CVF International Conference on Computer Vision (ICCV)*, October 2019. **1, 2**
- [13] Rohit Girdhar, Alaaeldin El-Nouby, Mannat Singh, Kalyan Vasudev Alwala, Armand Joulin, and Ishan Misra. Omnimae: Single model masked pretraining on images and videos. volume abs/2206.08356, 2022. **1**
- [14] Rohit Girdhar, Mannat Singh, Nikhila Ravi, Laurens van der Maaten, Armand Joulin, and Ishan Misra. Omnivore: A single model for many visual modalities. In *Proceedings of the IEEE/CVF Conference on Computer Vision and Pattern Recognition (CVPR)*, pages 16102–16112, June 2022. **1, 2**
- [15] Kensho HARA. Recent advances in video action recognition with 3d convolutions. *IEICE Transactions on Fundamentals of Electronics, Communications and Computer Sciences*, advpub:2020IMP0012, 2020. **1**
- [16] Kensho Hara, Hirokatsu Kataoka, and Yutaka Satoh. Can spatiotemporal 3d cnns retrace the history of 2d cnns and imagenet? In *Proceedings of the IEEE Conference on Computer Vision and Pattern Recognition (CVPR)*, June 2018. **1**
- [17] Ryota Hashiguchi and Toru Tamaki. Temporal cross-attention for action recognition. In *Proceedings of the Asian Conference on Computer Vision (ACCV) Workshops*, pages 276–288, December 2022. **1, 2, 3**
- [18] Kaiming He, Xiangyu Zhang, Shaoqing Ren, and Jian Sun. Deep residual learning for image recognition. In *Proceedings of the IEEE conference on computer vision and pattern recognition*, pages 770–778, 2016. **1**
- [19] Andrej Karpathy, George Toderici, Sanketh Shetty, Thomas Leung, Rahul Sukthankar, and Li Fei-Fei. Large-scale video classification with convolutional neural networks. In *Proceedings of the IEEE Conference on Computer Vision and Pattern Recognition (CVPR)*, June 2014. **1**
- [20] Will Kay, João Carreira, Karen Simonyan, Brian Zhang, Chloe Hillier, Sudheendra Vijayanarasimhan, Fabio Viola, Tim Green, Trevor Back, Paul Natsev, Mustafa Suleyman, and Andrew Zisserman. The kinetics human action video dataset. *CoRR*, abs/1705.06950, 2017. **3**
- [21] Yu Kong and Yun Fu. Human action recognition and prediction: A survey. *International Journal of Computer Vision*, 130(5):1366–1401, may 2022.
- [22] Alex Krizhevsky. Learning multiple layers of features from tiny images. Technical report, 2009. **3**
- [23] Alex Krizhevsky, Ilya Sutskever, and Geoffrey E Hinton. Imagenet classification with deep convolutional neural networks. In F. Pereira, C.J. Burges, L. Bottou, and K.Q. Weinberger, editors, *Advances in Neural Information Processing Systems*, volume 25. Curran Associates, Inc., 2012. **1**
- [24] Hildegard Kuehne, Hueihan Jhuang, Estíbaliz Garrote, Tomaso A. Poggio, and Thomas Serre. HMDB: A large video database for human motion recognition. In Dimitris N. Metaxas, Long Quan, Alberto Sanfeliu,

- and Luc Van Gool, editors, *IEEE International Conference on Computer Vision, ICCV 2011, Barcelona, Spain, November 6-13, 2011*, pages 2556–2563. IEEE Computer Society, 2011. **1**
- [25] Y. Lecun, L. Bottou, Y. Bengio, and P. Haffner. Gradient-based learning applied to document recognition. *Proceedings of the IEEE*, 86(11):2278–2324, 1998. **1**
- [26] Ang Li, Meghana Thotakuri, David A. Ross, João Carreira, Alexander Votrikov, and Andrew Zisserman. The ava-kinetics localized human actions video dataset. *CoRR*, abs/2005.00214, 2020. **1**
- [27] Valerii Likhoshervstov, Anurag Arnab, Krzysztof Choroński, Mario Lucic, Yi Tay, Adrian Weller, and Mostafa Dehghani. Polyvit: Co-training vision transformers on images, videos and audio. *CoRR*, abs/2111.12993, 2021. **1, 2, 3, 4**
- [28] Ji Lin, Chuang Gan, and Song Han. Tsm: Temporal shift module for efficient video understanding. In *Proceedings of the IEEE/CVF International Conference on Computer Vision (ICCV)*, October 2019. **1**
- [29] Ze Liu, Yutong Lin, Yue Cao, Han Hu, Yixuan Wei, Zheng Zhang, Stephen Lin, and Baining Guo. Swin transformer: Hierarchical vision transformer using shifted windows. In *Proceedings of the IEEE/CVF International Conference on Computer Vision (ICCV)*, pages 10012–10022, October 2021. **1**
- [30] Ze Liu, Jia Ning, Yue Cao, Yixuan Wei, Zheng Zhang, Stephen Lin, and Han Hu. Video swin transformer. In *Proceedings of the IEEE/CVF Conference on Computer Vision and Pattern Recognition (CVPR)*, pages 3202–3211, June 2022. **4**
- [31] Ilya Loshchilov and Frank Hutter. Decoupled weight decay regularization. In *7th International Conference on Learning Representations, ICLR 2019, New Orleans, LA, USA, May 6-9, 2019*. OpenReview.net, 2019. **3**
- [32] Daniel Neimark, Omri Bar, Maya Zohar, and Dotan Asselmann. Video transformer network. In *Proceedings of the IEEE/CVF International Conference on Computer Vision (ICCV) Workshops*, pages 3163–3172, October 2021. **1, 4**
- [33] Kazuki Omi, Jun Kimata, and Toru Tamaki. Model-agnostic multi-domain learning with domain-specific adapters for action recognition. *IEICE Transactions on Information and Systems*, E105-D(12):2119–2126, 2022. **3**
- [34] Zhaofan Qiu, Ting Yao, and Tao Mei. Learning spatiotemporal representation with pseudo-3d residual networks. In *Proceedings of the IEEE International Conference on Computer Vision (ICCV)*, Oct 2017. **1**
- [35] Javier Selva, Anders S. Johansen, Sergio Escalera, Kamal Nasrollahi, Thomas B. Moeslund, and Albert Clapés. Video transformers: A survey. *CoRR*, abs/2201.05991, 2022. **1**
- [36] Gilad Sharir, Asaf Noy, and Lihz Zelnik-Manor. An image is worth 16x16 words, what is a video worth? *CoRR*, abs/2103.13915, 2021. **1, 4**
- [37] Karen Simonyan and Andrew Zisserman. Two-stream convolutional networks for action recognition in videos. In Z. Ghahramani, M. Welling, C. Cortes, N. Lawrence, and K.Q. Weinberger, editors, *Advances in Neural Information Processing Systems*, volume 27. Curran Associates, Inc., 2014. **1**
- [38] Karen Simonyan and Andrew Zisserman. Very deep convolutional networks for large-scale image recognition. In Yoshua Bengio and Yann LeCun, editors, *3rd International Conference on Learning Representations, ICLR 2015, San Diego, CA, USA, May 7-9, 2015, Conference Track Proceedings*, 2015. **1**
- [39] Khurram Soomro, Amir Roshan Zamir, and Mubarak Shah. UCF101: A dataset of 101 human actions classes from videos in the wild. *CoRR*, abs/1212.0402, 2012. **1, 3**
- [40] Swathikiran Sudhakaran, Sergio Escalera, and Oswald Lanz. Gate-shift networks for video action recognition. In *IEEE/CVF Conference on Computer Vision and Pattern Recognition (CVPR)*, June 2020. **1**
- [41] Christian Szegedy, Wei Liu, Yangqing Jia, Pierre Sermanet, Scott Reed, Dragomir Anguelov, Dumitru Erhan, Vincent Vanhoucke, and Andrew Rabinovich. Going deeper with convolutions. In *2015 IEEE Conference on Computer Vision and Pattern Recognition (CVPR)*, pages 1–9, 2015. **1**
- [42] Du Tran, Lubomir Bourdev, Rob Fergus, Lorenzo Torresani, and Manohar Paluri. Learning spatiotemporal features with 3d convolutional networks. In *Proceedings of the IEEE International Conference on Computer Vision (ICCV)*, December 2015. **1**
- [43] Du Tran, Heng Wang, Lorenzo Torresani, Jamie Ray, Yann LeCun, and Manohar Paluri. A closer look at spatiotemporal convolutions for action recognition. In *Proceedings of the IEEE Conference on Computer Vision and Pattern Recognition (CVPR)*, June 2018. **1, 2**
- [44] Ashish Vaswani, Noam Shazeer, Niki Parmar, Jakob Uszkoreit, Llion Jones, Aidan N Gomez, Łukasz Kaiser, and Illia Polosukhin. Attention is all you need. **30**, 2017. **1**
- [45] Yufei Wang, Du Tran, and Lorenzo Torresani. Unidual: A unified model for image and video understanding. *CoRR*, abs/1906.03857, 2019. **2**
- [46] Saining Xie, Chen Sun, Jonathan Huang, Zhuowen Tu, and Kevin Murphy. Rethinking spatiotemporal feature learning: Speed-accuracy trade-offs in video classification. In *Proceedings of the European Conference on Computer Vision (ECCV)*, September 2018. **1, 3**
- [47] Hao Zhang, Yanbin Hao, and Chong-Wah Ngo. Token shift transformer for video classification. In *Proceedings of the 29th ACM International Conference on Multimedia*, MM '21, page 917–925, New York, NY, USA, 2021. Association for Computing Machinery. **1, 2, 3**
- [48] Yi Zhu, Xinyu Li, Chunhui Liu, Mohammadreza Zolfaghari, Yuanjun Xiong, Chongruo Wu, Zhi Zhang, Joseph Tighe, R. Manmatha, and Mu Li. A comprehensive study of deep video action recognition. *CoRR*, abs/2012.06567, 2020. **1**